Langebach, Jan ; Fischer, Peter; Karcher, Christian

Convective heat transfer of internal electronic components in a headlight geometry

URN: urn:nbn:de:gbv:ilm1-2016200146

Original published in:

World Academy of Science, Engineering and Technology : International Journal of Mechanical, Aerospace, Industrial, Mechatronic and Manufacturing Engineering, [Istanbul : WASET], 1 (2007), 4, p. 177-182.

ISSN (online): 2010-3778
ISSN (print): 2070-3724
URL: http://scholar.waset.org/1999.8/4676
[*Visited:* 2016-09-01]

Convective Heat Transfer of Internal Electronic Components in a Headlight Geometry

Jan Langebach, Peter Fischer, and Christian Karcher

***Abstract*—**A numerical study is presented on convective heat transfer in enclosures. The results are addressed to automotive headlights containing new-age light sources like Light Emitting Diodes (LED). The heat transfer from the heat source (LED) to the enclosure walls is investigated for mixed convection as interaction of the forced convection flow from an inlet and an outlet port and the natural convection at the heat source. Unlike existing studies, inlet and outlet port are thermally coupled and do not serve to remove hot fluid. The input power of the heat source is expressed by the Rayleigh number. The internal position of the heat source, the aspect ratio of the enclosure, and the inclination angle of one wall are varied. The results are given in terms of the global Nusselt number and the enclosure Nusselt number that characterize the heat transfer from the source and from the interior fluid to the enclosure walls, respectively. It is found that the heat transfer from the source to the fluid can be maximized if the source is placed in the main stream from the inlet to the outlet port. In this case, the Reynolds number and heat source position have the major impact on the heat transfer. A disadvantageous position has been found where natural and forced convection compete each other. The overall heat transfer from the source to the wall increases with increasing Reynolds number as well as with increasing aspect ratio and decreasing inclination angle. The heat transfer from the interior fluid to the enclosure wall increases upon decreasing the aspect ratio and increasing the inclination angle. This counteracting behaviour is caused by the variation of the area of the enclosure wall. All mixed convection results are compared to the natural convection limit.

***Keywords*—**Enclosure, heat source, heat transfer, mixed convection.

I. Introduction

THE problem of natural convection heat transfer in simple enclosures is extensively discussed in the literature. The most popular examples are the Rayleigh Bernard cell and enclosures with vertically heated and cooled walls. Such geometries are summarized by Ostrach [1] and Catton [2]. Natural convection in enclosures containing internal sources of different shape is investigated by Barozzi and Corticelli [3], Dong and Li [4] and Sun and Emery [5]. All of them use adiabatic horizontal walls and cooling/heating sidewalls. Mixed convection in enclosures with inlet and outlet ports are discussed due to the application in electronics cooling, e.g. enclosures containing electrical circuits. A variety of studies is provided by Papanicolaou and Jaluria [6]-[8]. They investigate an enclosure of constant shape with inlet and outlet port, while varying the position of the heat source, the conductivity of the source mounting frame and the finite thickness of the enclosure sidewalls. The heat is removed by the fluid flow from the inlet to the outlet ports. The enclose walls are considered as adiabatic.

The present work studies convection heat transfer of internal heat sources in automotive headlights. In comparison to existing studies of this kind, all heat is transferred through the enclosure walls, since inlet and outlet port are thermally coupled. So the influence of the enclosure shape, such as the aspect ratio and the inclination angle of one wall is investigated in detail. Section II of the paper introduces the simplified geometry and the solution parameters. Section III presents the results and discusses the findings. The paper is summarized in section IV.

II. Experimental Setup and Parameter Variation

A. Setup

The schematic sketch of the simplified headlight shows Fig. 1. All measures are indicated in Fig. 2. The two-dimensional enclosure is the cross section of a typical automotive headlight. The enclosure walls are kept at a constant temperature T_G. One of the vertical walls is inclined with the angle γ to the vertical direction. It represents the transparent lens of the automotive headlight. Since the height of the enclosure is fixed, its length is expressed by the aspect ratio $\Gamma = L/H$. Both, the inclination angle and the aspect ratio influence the overall area of the enclosure walls A_G. The bottom wall of the enclosure contains the inlet and outlet ports. Their location is fixed to the respective adjacent walls as well as their length E. Fluid enters the enclosure through the inlet port assuming a parabolic velocity profile with a mean velocity v and the inlet temperature T_L. The fluid leaves the model through the outlet port. Both, inlet temperature T_L and outlet temperature T_O are thermally coupled which yields: $T_L = T_O$. The absolute measures of the enclosure are H = 200mm and E = 35mm. Inside the enclosure a heat source is

Manuscript received May 25, 2007. This work was supported in part by the Automotive Lighting Reutlingen GmbH.

J. Langebach is with the Department for Mechanical Engineering, Technische Universität Ilmenau, P.O. Box 100 565, 98684 Ilmenau, Germany (phone: +49-3677-692465; fax: +49-3677-691214; e-mail: jan.langebach@tu-ilmenau.de).

P. Fischer, is with Automotive Lighting Reutlingen GmbH, Tübinger Str. 123, 72762 Reutlingen, Germany (e-mail: peter.fischer@al-lighting.com).

Ch. Karcher is with the Department for Mechanical Engineering, Technische Universität Ilmenau, P.O. Box 100565, 98684 Ilmenau, Germany (e-mail: christian.karcher@tu-ilmenau.de).

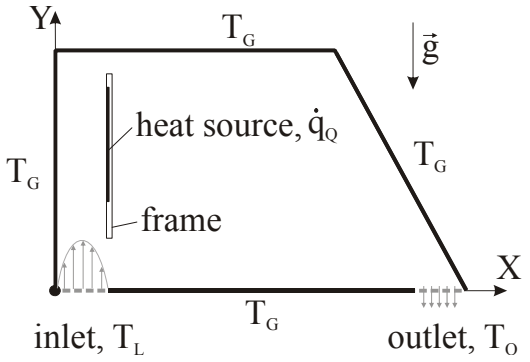

Fig. 1 Schematic draw of the headlight geometry

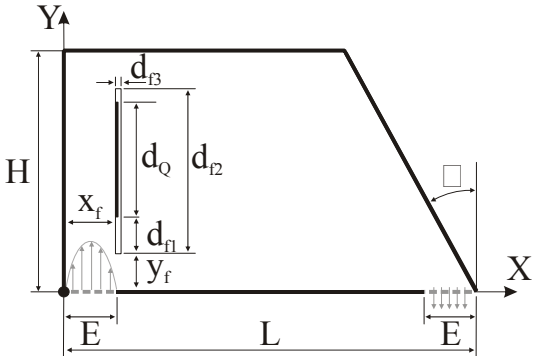

Fig. 2 Measures of the headlight geometry

placed and varied at six different positions. The source is mounted on an adiabatic frame with the thickness d_{f3} = 2mm and the height d_{f2} = 110mm. The position of the source is d_{f1} = 40mm above the lower edge of the frame and its height is d_Q = 60mm. The horizontal position $X_f = x_f/H$ and vertical position $Y_f = y_f/H$ of the frame is changed according to Table I.

TABLE I
HEAT SOURCE POSITIONS

Position	$X_f = x_f / H$	$Y_f = y_f / H$
1	0.175	0
2	0.175	0.250
3	0.175	0.400
4	0.400	0.000
5	0.400	0.250
6	0.400	0.400

A constant heat flux density $\dot{q}_Q$ is applied to the heat source. Depending on the heat transfer the source temperature $\overline{T}_Q$ is determined. This temperature is an area-average over the entire surface of the heat source A_Q.

B. Solution and Characteristic Numbers

The numerical solution is calculated by the finite volume code FLUENT™ version 6.2. For the current model the incompressible, steady state, two-dimensional governing equations are solved for the velocity $\vec{v}$, the density ρ, the temperature T and the fluid pressure p:

$$\begin{aligned} \nabla(\rho\vec{v}) &= 0 \\ \nabla(\rho\vec{v}) + \nabla(\rho\vec{v}\vec{v}) &= -\nabla p + \mu\nabla^2\vec{v} + (\rho - \rho_\infty)\vec{g} \\ c_p\nabla(\vec{v}\cdot\rho T) &= k\nabla^2 T \end{aligned} \qquad (1)$$

The dynamic viscosity μ, the heat capacity c_p, and the thermal conductivity k are assumed to be isotropic. The energy equation and momentum equation are coupled using the ideal gas approximation $\rho = p \cdot R/(M \cdot T)$, where M denotes the molar weight of air and R denotes the gas constant of air.

According to Papanicolaou and Jaluria [8] and Schlichting [9], for Re > 1700 the standard k-ε turbulence model according to Launder and Spalding [10] together with the enhanced wall function approach is used for the calculations. This is a standard turbulence approach in FLUENT™.

After calculating all values they are converted into characteristic numbers for heat and fluid flow. The forced convection is represented by the Reynolds number using the inlet length E as characteristic length and the average velocity $\bar{v}$ according to the pipe flow:

$$\mathrm{Re} = \frac{\bar{v} \cdot E \cdot \rho_L}{\mu}. \qquad (2)$$

In order to get a smooth fading from laminar to turbulent calculations, the values of the turbulent intensity is chosen to be nearly zero at the inlet port. This yields a turbulent viscosity being much smaller than the dynamic viscosity.

Since the ideal gas law is used to calculate the density ρ_L in equation (2) is calculated from the air temperature T_L.

To characterize natural convection, the Grashof number is used:

$$\mathrm{Gr} = \frac{g \cdot \beta \cdot \dot{q}_Q \cdot E^4}{k \cdot (\mu/\rho_L)^2}. \qquad (3)$$

The Nusselt number characterizes the heat transfer at the walls and is divided into the overall Nusselt number $\overline{\mathrm{Nu}}_{QG}$ denoting the heat transfer from the source to the enclosure walls and the enclosure Nusselt number $\overline{\mathrm{Nu}}_{LG}$ denoting the heat transfer from the fluid to the enclosure walls:

$$\overline{\mathrm{Nu}}_{QG} = \dot{q}_Q \cdot E/[k \cdot (\overline{T}_Q - T_G)] \qquad (5)$$

$$\overline{\mathrm{Nu}}_{LG} = \dot{q}_Q \cdot E/[k \cdot (T_L - T_G)]. \qquad (6)$$

C. Parameter Variation

During the present investigation we vary the Reynolds number, the Grashof number, the inclination angle, and the aspect ratio for each single heat source position as listed in Table II.

TABLE II
PARAMETER VARIATION

Parameter	Variation
Position	1 to 6 (see table I)
Re	190 … 4050
Gr	$1.3 \cdot 10^6$, $9.5 \cdot 10^6$
γ	0°, 20°, 45°
Γ	1.00, 1.11,1.25, 1.43, 1.67, 2.00

III. RESULTS AND DISCUSSION

At first the influence of the mixed convection is discussed. Later a comparison to the heat transfer by natural convection is given.

The flow from the inlet to the outlet port causes a main flow through the enclosure. Secondary eddies exist in dependence of the enclosure shape besides the main flow. They depend on the enclosure parameters inclination angle and aspect ratio. Details are given in the respective subsections.

A. Heat Source Position

Fig. 4 shows exemplarily the streamlines inside the enclosure for position 4 and 5 of the heat source. The Reynolds number for the Fig. is approx. Re ≈ 4050. For position 5, the source is placed in-between the main flow. The direction of the buoyancy force and the momentum force matches at the source which is the case for all Reynolds numbers. For position 4, the source is located below the main stream. Viscous forces of the main stream drive an eddy which rotates against the buoyancy force at the source.

Regarding the heat transfer in terms of the Nusselt number, these two positions delimit the possible minimum and maximum heat transfer. Generally, the interaction of the main flow MF and the flow at the heat source HF interact in three ways:

1. HF and MF are identical.
2. MF does not meet the source but viscous driven eddies cause a HF which is supporting the buoyancy force.
3. MF does not meet the source and viscous driven eddies retard the HF.

NOMENCLATURE

Symbol	Quantity	Unit
A	area	m²
c_p	specific heat capacity	J/kg K
E	inlet/outlet width	m
g	acceleration of gravity	m/s²
Gr	Grashof-number	
H	enclosure height	m
k	thermal conductivity	W/m K
L	enclosure length	m
M	molecular weight	kg/mol
$\overline{Nu}$	area-averaged Nusselt number	
p	pressure	Pa
$\dot{q}$	heat flux density	W/m²
R	gas constant	J/mol K
Re	Reynolds number	
T	temperature	K
$\overline{T}$	area-averaged temperature	K
$\vec{v} = (u, v)$	velocity	m/s
$\overline{v}$	area-averaged velocity	m/s
$\vec{x} = (x, y)$	location	m
$\vec{X} = (X, Y)$	normalized location	
β	thermal expansion coefficient	1/K
Γ	aspect ratio	
γ	inclination angle of enclosure wall	°
μ	dynamic viscosity	Pa s
ρ	density	kg/m³
subscripts:		
f	frame	
G	enclosure wall	
L	inlet value	
LG	interior air to enclosure	
O	outlet value	
Q	source	
QG	source to enclosure	

This behaviour depends on the Reynolds number.

Fig. 5 shows the overall Nusselt number $\overline{\mathrm{Nu}}_{\mathrm{QG}}$ for all positions of the heat source. For low Reynolds numbers, the retarding effect of the viscous driven eddy at the heat source position 4 causes a reduction of the Nusselt number. The momentum force of the eddy exceeds the buoyancy force for higher Reynolds numbers and the Nusselt number rises due to

(a) position 4 (b) position 5

Fig. 4 Streamlines inside the enclosure for different positions. Gr = $1.3 \cdot 10^6$, Re ≈ 4050, Γ = 1.25, γ = 20°

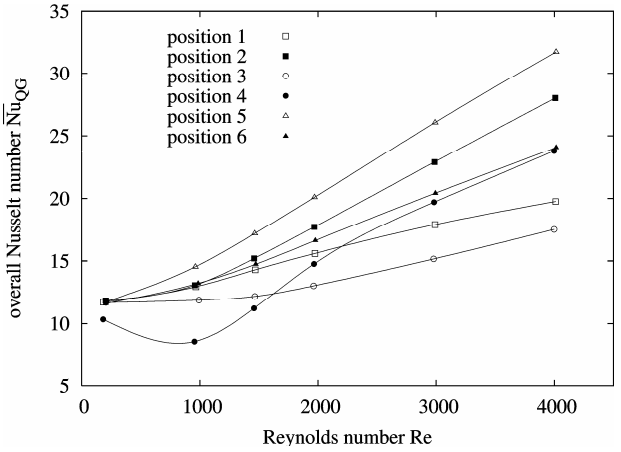

Fig. 5 Overall Nusselt number in dependence of the Reynolds number for different positions of the heat source. $\Gamma = 1.25$, $\gamma = 20°$, $Gr = 9.5 \cdot 10^6$

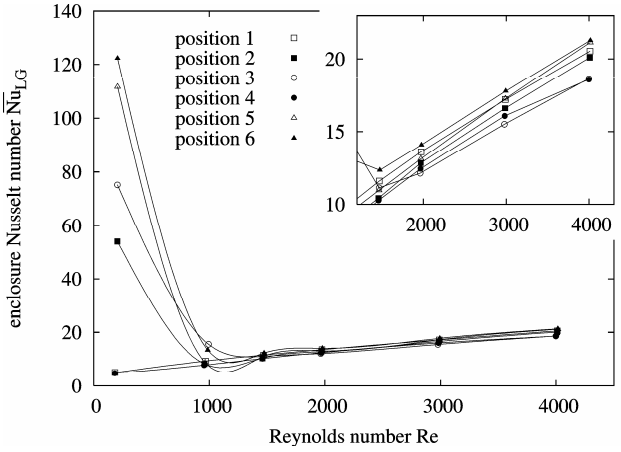

Fig. 6 Enclosure Nusselt number in dependence of the Reynolds number for different positions of the heat source. $\Gamma = 1.25$, $\gamma = 20°$, $Gr = 9.5 \cdot 10^6$

the forced convection. In all other positions the Nusselt number increases while increasing the Reynolds number. Their slope depends on the interaction of the HF and the MF.

The enclosure Nusselt number $\overline{Nu}_{LG}$ in Fig. 6 shows also a dependence of the source position for high Reynolds numbers, but it differs from the behaviour of the overall Nusselt number. For the enclosure, position 5 and 6 achieve maximum heat transfer. In these cases, the MF is guided to the enclosure walls by the heat source itself enhancing the heat transfer at the enclosure walls. This effect is only possible for configurations where the MF meets the heat source such like position 5 and 6.

For low Reynolds numbers, the MF inside the enclosure exists apart from the HF. Both do not interact for positions like 2, 3, 5 and 6. Therefore, the moving fluid from the inlet to the outlet ports stays at low temperature which misleadingly results in very high enclosure Nusselt numbers in Fig. 6. In position 1 and 4 the heat source is even for small Reynolds numbers in touch with the MF. Therefore, the enclosure Nusselt number increases monotonically with the Reynolds number.

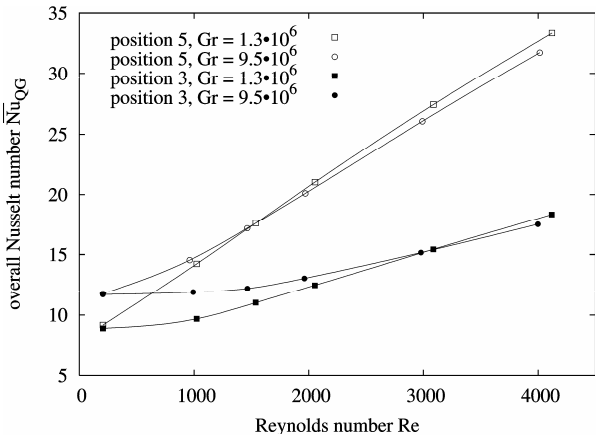

Fig. 7 Overall Nusselt-number in dependence of the Reynolds-number and Grashof number for different positions of the heat source. $\Gamma = 1.25$, $\gamma = 20°$

B. *Grashof Number*

The streamlines are less-influenced by the Grashof number. Only for position 4 its effect on the development of the eddy at the heat source is observable. The comparison $Gr = Re^2$ yields $Re \approx 1140$ for $Gr = 1.3 \cdot 10^6$ and $Re \approx 3080$ for $Gr = 9.5 \cdot 10^6$ where buoyancy and momentum forces have the same order of magnitude which is indicated by the intersection of the curves in the Fig. Due to buoyancy, the overall Nusselt number rises upon increasing Gr for small Re. For high Reynolds numbers, only small a dependence on the Grashof number is observable since the heat transfer is driven by momentum forces. Due to the local variation of the air temperature inside the enclosure, the local density $\rho(X,Y)$ varies as well. Thereby, the local Reynolds number is lowered reducing the heat transfer. Since the Reynolds number is calculated at the inlet port according to the temperature T_L, local variations of Re are not included. They cause a slight reduction of the overall Nusselt number for high Reynolds numbers. This behaviour is limited to the heat transfer from the source to the fluid and is not observable for the enclosure Nusselt number.

C. *Inclination Angle and Aspect Ratio*

The streamline plots for the variation of the enclosure shape, namely the inclination angle and the aspect ratio are shown in Fig. 8. The inclination angle is changed in the first column for a constant aspect ratio $\Gamma = 1.0$ and the aspect ratio is changed in the second column for a constant inclination angle $\gamma = 20°$. The plots are taken for a constant Grashof number of $Gr = 9.5 \cdot 10^6$, a Reynolds number $Re \approx 4050$, and heat source position 5. If the heat source position remains constant, the streamlines do not change significantly between the inlet port and the heat source as indicated in the Fig. Only if the enclosure size is strongly reduced a small effect on the streamlines in this area is observable. In the region between the heat source and the outlet port the flow is always influenced by the shape of the enclosure. The bigger the inclination angle is the easier the flow attaches to the

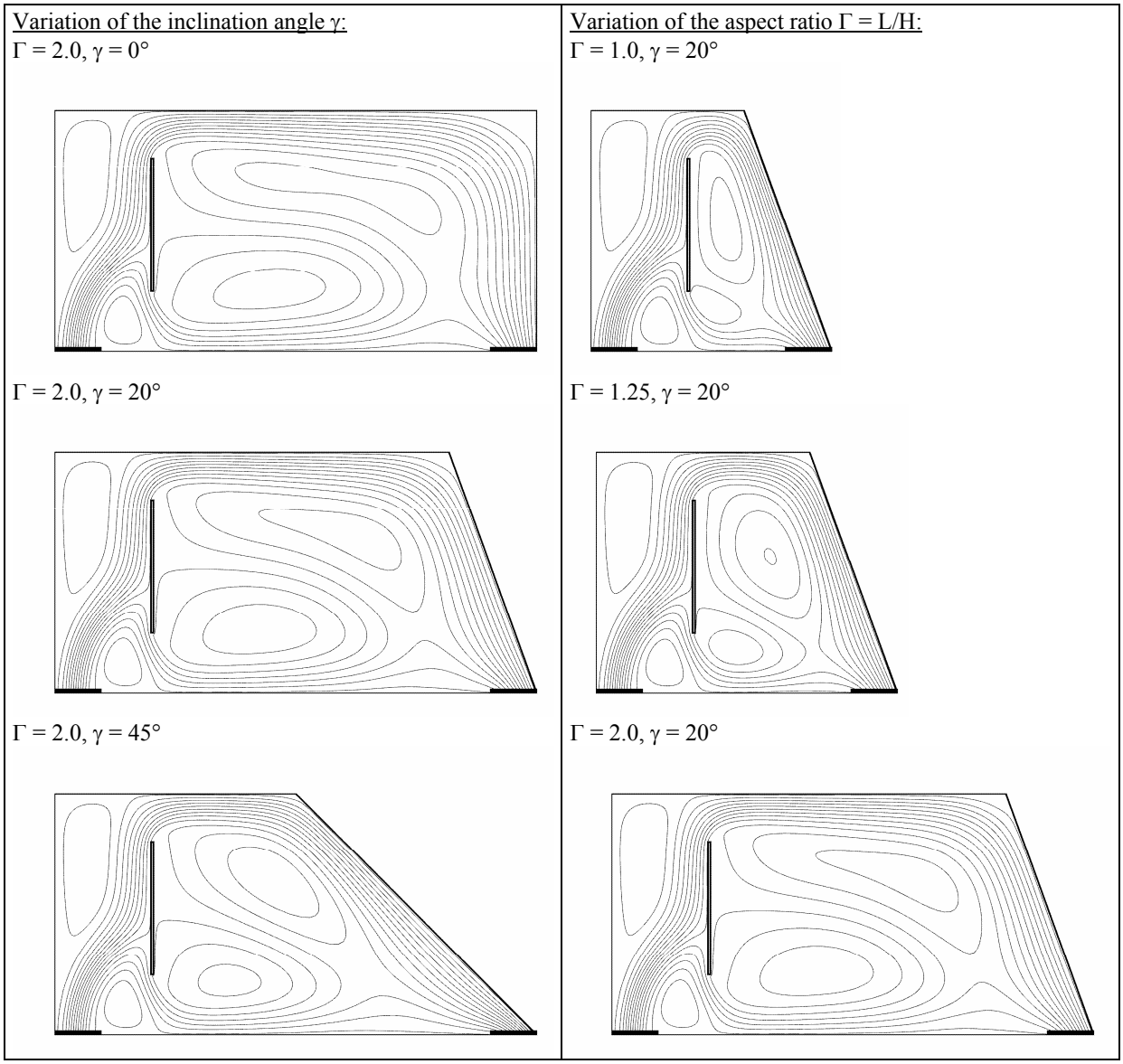

Fig. 8 Streamlines for the variation of the aspect ratio Γ and the inclination angle γ. Gr = $9.5 \cdot 10^6$, Re ≈ 4050, heat source position 5

enclosure walls. The aspect ratio effects the development of eddies in the core area between heat source and outlet port. Two counterrotating eddies exist for big aspect ratios. The smaller the aspect ratio is the more disappears the lower eddy.

Fig. 9 shows the influence of the inclination angle and aspect ratio on the overall Nusselt number. The aspect ratio remains constant in groups marked by double-head arrows. The biggest aspect ratio is on the left, the lowest ratio is on the right. In each group of constant aspect ratio the inclination angle is increased in the direction of the arrows which means from the left to the right side, respectively. Fig. 9 reveals that the smaller the aspect ratio is the smaller the overall Nusselt number is. Moreover, the Nusselt number reduces upon increasing the inclination angle.

As mentioned in the experiment description the inclination angle and the aspect ratio influence the total area of the enclosure walls A_G. The ratio of the heat source area A_Q to the enclosure area A_G is shown on the abscissa of Fig. 9. It changes from 0.053 to 0.09 during the entire investigation. The overall Nusselt number follows a specific trend in dependence of A_Q/A_G: The higher the ratio of the heat source area to the enclosure area is the lower is the overall Nusselt number. This is caused by the reduction of the heat transferring area of the enclosure.

Fig. 10 shows the enclosure Nusselt number for Re ≈ 4050 in dependence of the aspect ratio and the inclination angle in an enclosure without a heat source. As indicated the Nusselt number is increasing upon decreasing the aspect ratio. The higher the aspect ratio is the larger is the space available for the mean flow and the smaller is the velocity gradient at the wall. Fig. 10 also shows that higher inclination angles increase the enclosure Nusselt number. This is due to the better flow attachment to the enclosure walls. Both, the enclosure Nusselt number and the ratio of the heat source area to enclosure area

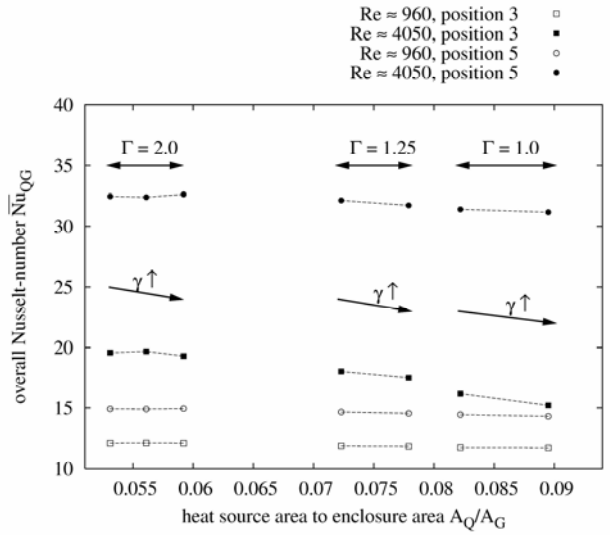

Fig. 9 Overall Nusselt number in dependence of the ratio A_Q/A_G representing different aspect ratios Γ and inclination angles γ. Gr = $9.5 \cdot 10^6$

influence the overall Nusselt number. Since the ratio A_Q/A_G doubles during the parameter variation its influence exceeds the increasing enclosure Nusselt number. Therefore, the overall Nusselt number does not benefit of the improved enclosure Nusselt number.

The curves in Fig. 10 show local minima or maxima for small aspect ratios, especially for γ = 20°. For small aspect ratios the MF does not attach to the upper wall anymore. An eddy is forming in the upper part of the enclosure and changes the enclosure Nusselt number. If a heat source is inserted, the development of this eddy is prevented, but the trend of Fig. 10 in dependence of Γ and γ stays valid.

D. Natural Convection Limit

The overall Nusselt number for natural convection is less influenced by the heat source position. The values of the overall Nusselt number are approx. 9.0 for Gr = $1.3\ 10^6$ and 11.9 for Gr = $9.5\ 10^6$ and does not differ very much from the values for Re ≈ 190 shown in Fig. 7. The enclosure shape has similar influences as discussed in the previous subsection. The significant parameter is the ratio A_Q/A_G.

The overall Nusselt number is more than doubled from natural convection to mixed convection in the present investigation.

IV. Summary and Conclusion

A study on the heat transfer of electronic components in headlights is presented. The forced flow of one inlet and one outlet port is thermally coupled. The overall Nusselt number and the enclosure Nusselt number are used to express the heat transfer from the heat source to the wall. The effect of the Reynolds number, the Grashof number, the heat source position as well as the enclosure parameters inclination angle and aspect ratio are investigated. The results show that both Nusselt numbers increase upon increasing the Reynolds number except for heat source positions, where natural and

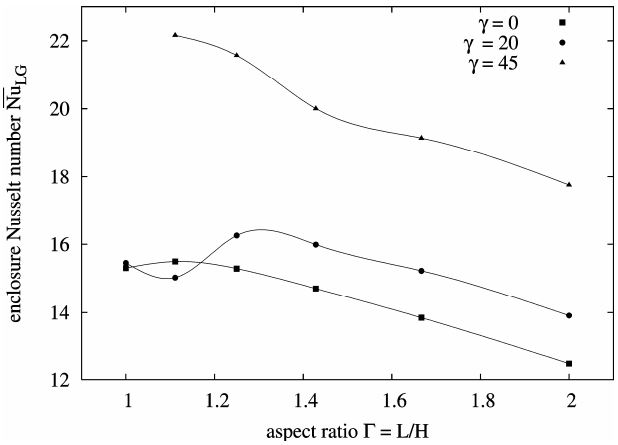

Fig. 10 Enclosure Nusselt number in dependence of the aspect ratio Γ and the inclination angle γ for an empty enclosure (without heat source). Re = 3800

forced convection compete. The Reynolds number has the biggest effect of all investigated parameters. The Grashof number is found to increase the heat transfer especially for small Reynolds numbers. This effect ceases for high Reynolds numbers. Remarkable improvement of the heat transfer can be achieved with the heat source position. If it is positioned in the mean flow the heat transfer is maximized. Changing the enclosure shape by inclination angle and aspect ratio in the way that the enclosure area is maximized yields a rise of the overall Nusselt number. Although the enclosure Nusselt number is decreasing in this case, its influence on the overall Nusselt number is rather low. Therefore, the influence of the Nusselt number at the heat source is much bigger than the influence of the enclosure Nusselt number.

References

[1] S. Ostrach, "Natural convection in enclosures", in *Advances in heat transfer*, vol. 8, Academic Press, 1972, pp. 161–227.

[2] I. Catton, "Natural convection in enclosures", *Proc. 6th Int. Heat Transfer Conference*, vol. 6, pp. 13–31, 1972.

[3] G. S. Barozzi, M. A. Corticelli, "Natural convection in cavities containing internal sources", *Heat Mass Transfer*, vol. 36, no. 6, pp. 473–480, 2000.

[4] S. F. Dong, Y. T. Li, "Conjugate of natural convection and conduction in a complicated enclosure", *Heat Mass Transfer*, vol. 47, pp. 2233–2239, 2004.

[5] Y. S. Sun, A. F. Emery, "Effects of wall conduction, internal heat sources and an internal baffle on natural convection heat transfer in a rectangular enclosure", *Int. J. Heat Mass Transfer*, vol. 40, no. 4, pp. 915–929, 1997.

[6] E. Papanicolaou, Y. Jaluria "Mixed convection from a localized heat source in a cavity with conducting walls: a numerical study", *Num. Heat Transfer A*, vol. 23, pp. 463–484, 1993.

[7] E. Papanicolaou, Y. Jaluria, "Mixed convection from simulated electronic components at varying relative positions in a cavity", *J. Heat Transfer*, vol. 116, pp. 960–970, 1994.

[8] E. Papanicolaou, Y. Jaluria, "computation of turbulent flow in mixed convection in a cavity with a localized heat source", *J. Heat Transfer*, vol. 117, pp. 649–658, 1995.

[9] H. Schlichting, K. Gersten, *Boundary-Layer Theory*, Berlin: Springer, 2000.

[10] B. E. Launder, D. B. Spalding, *Lectures in mathematical models of turbulence*, London: Academic Press, 1972.